Numerical simulation of an unsaturated flow equation *

XIE Zhenghui (谢正辉), ZENG Qingcun (曾庆存), DAI Yongjiu (戴永久)
and WANG Bin (王 斌)

(LASG, Institute of Atmospheric Physics, Chinese Academy of Sciences, Beijing 100080, China)

Received November 18, 1997

Abstract A numerical model for an unsaturated flow problem by using the finite element method is established in order to simulate liquid moisture flow in an unsaturated zone with homogeneous soil and deep subsurface water, and with different initial and boundary conditions. For infiltration or evaporation problems, a traditional method usually yields oscillatory non-physics profiles. However, nonoscillatory solutions are obtained and non-physics solutions for these problems are evaded by using the mass-lumped finite element method. Moreover, the kind of boundary condition is handled very well.

Keywords: unsaturated flow, finite element, mass lumping, numerical simulation.

Fluid movement in unsaturated soil is the flow where water is not full of hole, and is an important form of flow in porous media. Prediction of an unsaturated flow is provided with significance in many branches of science and engineering. These include atmospheric science, soil science, agricultural engineering, environment engineering, and groundwater hydrology. Soil moisture is an important climate factor, and its seasonal change plays important influence on weather and climate in mid-high latitude regions. Landsurface parameterization which stresses computation of soil moisture, is a popular problem[1,2]. Hydraulic processes at surface and subsurface, such as precipitation, evaporation, and evaporotranspiration, seepage of surface water, and capillary elevation of deep-level water, absorption in root zone and liquid moisture flow of groundwater, all can be reduced to unsaturated flow problems[3—7]. The numerical solutions for the finite difference method are very sensitive to infiltration or evaporation boundary conditions and soil parameters. The kind of boundary condition is handled very well through reducing to calculation of known flux by using variation. It is extremely possible to yield non-physics oscillatory infiltration or evaporation profiles by using the traditional finite element method. We obtain nonoscillatory solutions and evade oscillatory non-physics profiles by using the mass-lumped finite element method. It can be used in simulation of liquid moisture flow for infiltration, evaporation, evapotranspiration, re-distribution, and their alternate appearances.

1 A numerical model of one-dimensional unsaturated flow

1.1 Vertical infiltration and evaporation problems

Based on horizontal resolving power of AGCM (1—5 longitude-latitude), liquid moisture flow in soil along horizontal direction may be ignored. We consider one-dimensional unsaturated problems. Water head has different temporal-spatial distributions. Let z denote the vertical

* Project supported by the National Key Project of Fundamental Research "Climate Dynamics and Climate Prediction Theory" and China Postdoctoral Science Foundation.

© 1995-2004 Tsinghua Tongfang Optical Disc Co., Ltd. All rights reserved.

dimension, assumed positive downward, and $h(z, t)$ be water head at time t and at the distance z from surface. We suppose that the infiltration or evaporation rate at surface dependent on time is given, here that is positive for infiltration and negative for evaporation; groundwater lay hidden in the earth deeply, and does not reach the domain $\Omega = (0, L)$; water head or soil moisture at the bottom of the domain Ω is given dependent on time. Then by the Darcy law and the continuous principle, we obtain the following unsaturated flow Richard equation:

$$C(h)\frac{\partial h}{\partial t} - \frac{\partial}{\partial z}\left[K(h)\frac{\partial h}{\partial t}\right] + \frac{\partial K(h)}{\partial z} = S_r, \qquad (1.1)$$

where $C(h) = \partial\theta/\partial h[1/L]$ is the specific moisture capacity; $\theta[L^3/L^3]$, soil moisture; $h[L]$, water head; $K(h)[LT^{-1}]$, the unsaturated hydraulic conductivity; $S_r[L^3T^{-1}L^{-3}]$, absorption rate of root zone[3—9]. The presumed condition is as follows:

(i) initial condition: $h(z, 0) = h_0(z)$;

(ii) lower boundary condition: $h(L, t) = \beta(t)$;

(iii) upper boundary condition has the following cases:

Infiltration:

(a) If the known surface flux did not exceed the infiltration intensity, and did not generate runoff,

$$K(h) - K(h)\frac{\partial h}{\partial z} = q(t), \qquad \text{when } z = 0,$$

which is the second kind of boundary condition.

(b) If the known surface flux did not exceed the infiltration intensity until runoff had generated,

$$\begin{cases} K(h) - K(h)\dfrac{\partial h}{\partial z} = q(t), & \text{when } z = 0; \text{ and } t_a > t > 0 \\ h(0, t) = 0, & \text{when } t \geq t_a, \end{cases}$$

where t_a was the beginning time when it exceeded the infiltration strength, and was taken as the beginning time of $h(0, t) = 0$ since $h \leq 0$.

(c) If surface kept wet or thin-level water, $h(0, t) = 0$.

Evaporation:

(a) If soil at surface was evaporated at evaporation rate $q(t)$,

$$K(h) - K(h)\frac{\partial h}{\partial z} = q(t), \text{ at } z = 0,$$

where $q(t) \leq 0$.

(b) If soil at surface was evaporated at a high intensity and soil moisture at surface became the air-dried rate θ_d in a short time, $h(0, t) = h_d$.

(c) If soil at surface was evaporated at evaporation rate $q(t)$, and soil moisture at surface reached the air-dried rate after time t_a,

$$\begin{cases} K(h) - K(h)\dfrac{\partial h}{\partial z} = q(t), \text{when } z = 0, \text{ and } t_a > t > 0; \\ h(0, t) = h_d, \text{ when } z = 0, \text{ and } t > t_a; \end{cases}$$

here t_a was the beginning time when that reached the air-dried rate, and was taken as the beginning time of $h = h_d$ since $h \geq h_d$.

Re-distribution:

© 1995-2004 Tsinghua Tongfang Optical Disc Co., Ltd. All rights reserved.

If surface flux was zero,

$$K(h) - K(h)\frac{\partial h}{\partial z} = 0, \qquad \text{when} \qquad z = 0 \text{ and } t_a > t > 0,$$

which is the second kind of boundary condition.

According to the presumed conditions, we can solve the basic equation and obtain the water head distribution for vertical infiltration, evaporation, evaportranspiration, re-distribution, and their alternative appearances. And then the soil moisture distribution follows from the construction relation of h and θ.

As an example we consider eq. (1.1) with the initial condition and the low boundary condition mentioned above, and with the infiltration or evaporation upper boundary conditions, and explain numerical simulation processes of the model.

Let $H_E^1(\Omega) = \{ v \in H^1(\Omega), v(L) = 0 \}$, here $H^1(\Omega)$ is a Sobolev space, up to the first derivatives of which are square integrable[10] on Ω. Set $h(z,t) = \overline{h}(z,t) + \beta(t)$, and homogenize the lower boundary condition. Then the equivalent variational formulation of the considered problem (on $t \in (0, T)$) is as follows:

$$\begin{cases} \text{to find } h(z,t) \in H_E^1(\Omega), \ \forall t \in (0,T), \text{ such that } \forall \phi \in H_E^1(\Omega), \\ \left(C(h)\frac{\partial \overline{h}}{\partial t}, \phi \right) + \left(C(h)\frac{\partial \overline{h}}{\partial z}, \frac{\partial \phi}{\partial z} \right) = q\phi|_0^L + \int_0^L K(h)\frac{\partial \phi}{\partial z}\mathrm{d}z + (S_r, \phi) - \left(C(h)\frac{\partial \beta}{\partial t}, \phi \right), \end{cases} \tag{1.2}$$

where and from now on $(\cdot, \cdot)$ denotes the L^2-inner product on Ω[10].

1.2 Finite element approximations

1.2.1 Semi-discrete finite element approximation. We first introduce finite element approximation in space direction. Divide the domain $\Omega = (0, L)$ such that $0 = x_0 < x_1 < x_2 < \cdots < x_{n+1} = L$, where x_0 and x_{n+1} are the boundary points of domain Ω. Let $e_i = (x_i, x_{i+1})$ $(i = 0, \cdots, n)$ be $n+1$ elements. Define a finite element space $V_h \subset H_E^1(\Omega)$ such that $V_h = \{ v_h$ is continuous in $[0,1]$, $v_h|_{e_i}$ is linear polynomial for $0 \leq i \leq n$ and $v_h(L) = 0 \}$.

Let $\{\phi_i\} \subset V_h$ be the finite element basic functions[11], $\phi_i(x_j) = \delta_{ij}$ $(i, j = 0, \cdots, n+1)$. Since $\overline{h} \in V_h$, $h(z,t) = \sum_{i=0}^{n} X_i(t)\phi_i(x) + \beta(t)$. Therefore, the matrix formulation of semidiscrete finite element approximation of the problem (1.2) may be written as

$$\begin{cases} [A]\{X\} + [B]\left\{\frac{\mathrm{d}X}{\mathrm{d}t}\right\} = \{F\}, \\ \{X(0)\} = (h_0(x_0) - \beta(0), \cdots, h_0(x_n) - \beta(0))^{\mathrm{T}}, \end{cases} \tag{1.3}$$

where

$$\begin{cases} [A] = [A_{ij}], A_{ij} = \int_0^L K(h)\frac{\mathrm{d}\phi_i}{\mathrm{d}z}\frac{\mathrm{d}\phi_j}{\mathrm{d}z}\mathrm{d}z, \\ [B] = [B_{ij}], B_{ij} = \int_0^L C(h)\phi_i\phi_j\mathrm{d}z, \\ \{F\} = [F_i], F_i = q(h)\phi_i|_0^L + (S_r, \phi_i) - \int_0^L K(h)\frac{\mathrm{d}\phi_i}{\mathrm{d}z}\mathrm{d}z, \\ \{X\} = (X_0(t), \cdots, X_n(t))^{\mathrm{T}}, \\ \left\{\frac{\mathrm{d}X}{\mathrm{d}t}\right\} = \left(\frac{\mathrm{d}X_0}{\mathrm{d}t}, \cdots, \frac{\mathrm{d}X_n}{\mathrm{d}t}\right)^{\mathrm{T}}, i, j = 0, \cdots, n. \end{cases} \tag{1.4}$$

© 1995-2004 Tsinghua Tongfang Optical Disc Co., Ltd. All rights reserved.

Eq. (1.3) defines a set of ordinary differential equations with nonlinear coefficients. To get a numerical solution of the problem, discretization for time variable should be introduced.

1.2.2 A full discrete scheme. A finite difference scheme may be introduced to approximate the time derivatives in the matrix equation, and then the Galerkin finite element-finite difference scheme of problem (1.2) is obtained. Define for that purpose the following approximations:

$$\begin{cases} \left\{\frac{\mathrm{d}X}{\mathrm{d}t}\right\} \approx \frac{\{X\}^{t+\Delta t} - \{X\}^{t}}{\Delta t}, \\ \{X\}^{t+\Delta t/2} \approx \omega\{X\}^{t+\Delta t} + (1-\omega)\{X\}^{t}, \end{cases} \tag{1.5}$$

where Δt is the time step and ω a temporal weighting coefficient. By defining matrix equation (1.3) at the half-time level $(t+\Delta t/2)$, and introducing approximations in (1.5), the following algebraic equation system yields

$$[A]^{t+\Delta t/2}(\omega\{X\}^{t+\Delta t} + (1-\omega)\{X\}^{t}) + [B]^{t+\Delta t/2}\frac{\{X\}^{t+\Delta t} - \{X\}^{t}}{\Delta t} = \{F\}^{t+\Delta t/2}.$$

And then

$$[P]^{t+\Delta t/2}\{X\}^{t+\Delta t} = [Q]^{t+\Delta t/2}\{X\}^{t} + \{F\}^{t+\Delta t/2}, \tag{1.6}$$

where

$$\begin{cases} [P] = \omega[A] + \frac{1}{\Delta t}[B], \\ [Q] = (\omega-1)[A] + \frac{1}{\Delta t}[B]. \end{cases} \tag{1.7}$$

When $\omega = 1$ an implicit in time finite difference scheme results, even through the various coefficients are evaluated at the half-time level. When $\omega = 1/2$, on the other hand, a time-centred, Crank-Nicolson type algorithm is obtained. To be able to solve eq. (1.6), one needs estimates of the coefficients K and C and then coefficient matrix $[A], [B], [F]$ in eq. (1.4) and $[P], [Q]$ in eq. (1.6) at the half-time level. Since the mass-lumped finite element method is used in computation, and all elements in each row are summed up into the main-diagonal element, oscillatory non-physics profiles are evaded. Because elements of these matrix depend on the water head, it is necessary to have an estimate of the water head distribution h at the half-time level. For each new time step this distribution is obtained through linear extrapolation from the old distributions as follows:

$$h^{t+\Delta t/2} = h^{t} + \frac{\Delta t_{\mathrm{n}}}{2\Delta t_{\mathrm{o}}}(h^{t} - h^{t-\Delta t}), \tag{1.8}$$

where Δt_{n} and Δt_{o} are new and old time increments, respectively. Expression (1.5) is a kind of approximations, which may be improved by means of pre-estimate and correct iteration processes. During each iteration the most recent distribution of $h_0^{t+\Delta t}$, obtained by solving eq. (1.6), is used to obtain a new estimate for the half-time level: $h^{t+\Delta t/2} = (h_0^{t+\Delta t} + h^{t})/2$. By using $h^{t+\Delta t/2}$, a new water head $h_n^{t+\Delta t}$ may be obtained by solving eq. (1.6). The iterative process continues until a satisfactory degree of convergence is obtained. The criterion of convergence, in its most general form, is given by: $|h_n^{t+\Delta t} - h_0^{t+\Delta t}| \leq \mu_1 + \mu_2|h_n^{t+\Delta t}|$, where k represents the iteration number, and μ_1, μ_2 are the selected absolute and relative error criteria.

To compute water head distribution at a new time level, the first step is to estimate $h^{t+\Delta t/2}$ water head distribution at the half-time step. If the time level is not the first one, it can be

© 1995-2004 Tsinghua Tongfang Optical Disc Co., Ltd. All rights reserved.

pre-estimated through linear extrapolation according to (1.8). However, if the time level is the first one, it cannot do so since only initial distribution is known. In this case, the initial distribution may be taken as the pre-estimated distribution at the first half time level.

2 Numerical simulation

A series of infiltration experiments were done in the laboratory using a plexiglass column[7], 93.5-cm long and 6-cm inside diameter (ID) uniformly packed with sand to a bulk density of 1.66 g/cm^3. The column was equipped with tensiometers at depths of 7, 22, 37, 52, 67, and 82 cm below the soil surface. Each tensiometer had its own pressure transducer. The changes of water content at different depths were obtained by Gamma ray attenuation. A constant water head was maintained at the lower end of the column and a constant flux (13.96 cm/h) was imposed at the soil surface ($z = 0$) during 0.7 h since beginning of infiltration. Assume that after 0.7 h evaporation began at the evaporation rate 4mm/h; and when soil moisture at surface reached the air-dried rate, $h(0, t) = -61.5$ cm. The hydraulic conductivity-the water content relationship of the soil was obtained by analysis of the water-content and water head profiles during transient flow[8,9]. The soil-water head-water content relationship was obtained at each tensiometer depth by correlating tensioments readings and water-content measurements during the experiments[7]. The following analytical expressions obtained by a least square fit through all data points were chosen for characterizing this soil:

$$\begin{cases} K(h) = K_s \dfrac{A}{A + |h|^{\gamma}}, \quad K_s = 34 \text{ cm/h}, \quad A = 1.17 \times 10^6, \gamma = 4.74; \\ \theta(h) = \dfrac{\alpha(\theta_s - \theta_r)}{\alpha + |h|^{\beta}} + \theta_r, \quad \theta_s = 0.287, \ \theta_r = 0.075, \alpha = 1.611 \times 10^6, \beta = 3.96; \end{cases} \tag{2.1}$$

where dimension of h is cm, subscript s refers to saturation, i.e. the value of θ for which $h = 0$, and the subscript r to residual water content (see refs. [7,9]). The initial and boundary conditions for infiltration of water in the sand were

$$\begin{cases} h(0, z) = -61.5 \text{ cm (or } \theta_n = 0.10 \text{ cm}^3/\text{cm}^3), \ z \in [0, 70]; \\ q(t, 0) = \begin{cases} 13.69 \text{ cm/h}, & \text{when } 0 < t < 0.7 \text{ h}, \\ q = -0.4 \text{ cm/h}, & \text{when } t > 0.7 \text{ h}, \end{cases} \\ h(70, t) = -61.5 \text{ cm}. \end{cases} \tag{2.2}$$

Divide the domain $\Omega = (0, 70)$ into 70 elements. The time step $\Delta t = 5$s. Those data were included into the program. The obtained soil moisture profiles from 0 to 0.7 h, are presented in fig. 1. Here the ordinate denotes soil moisture, abscissa denotes depth from surface, and each curve denotes a soil moisture profile at certain time. By comparing the soil moisture profiles in fig. 1 with those of experiments done in ref. [7], we can find that the results are coincident. There are no oscillatory non-physics profiles for the monotone infiltration problem.

Figure 2 presents infiltration profiles at the initial stage (from 0.0 to 0.1h) and at each 0.1h period afterwards. It may be seen from fig. 2 that soil moisture at surface increased from 0.1 to 0.25 rapidly during 0.1h since infiltration occurring. After that time it changed a little and gradually approached the saturated soil moisture. When $t > 0.7$ h, soil at the surface was evaporated at intensity 4 mm/h, i.e. $q = -4$ mm/h. Fig. 3 presents soil moisture profiles at 0.7 h and at

© 1995-2004 Tsinghua Tongfang Optical Disc Co., Ltd. All rights reserved.

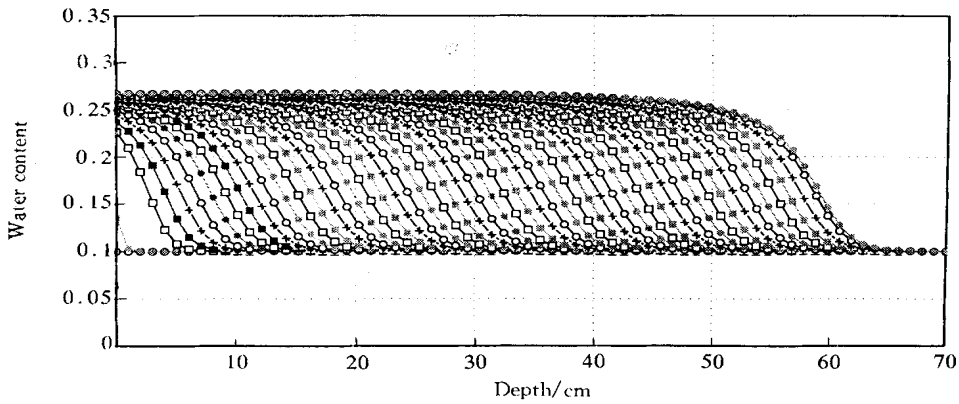

Fig. 1. Soil moisture profiles.

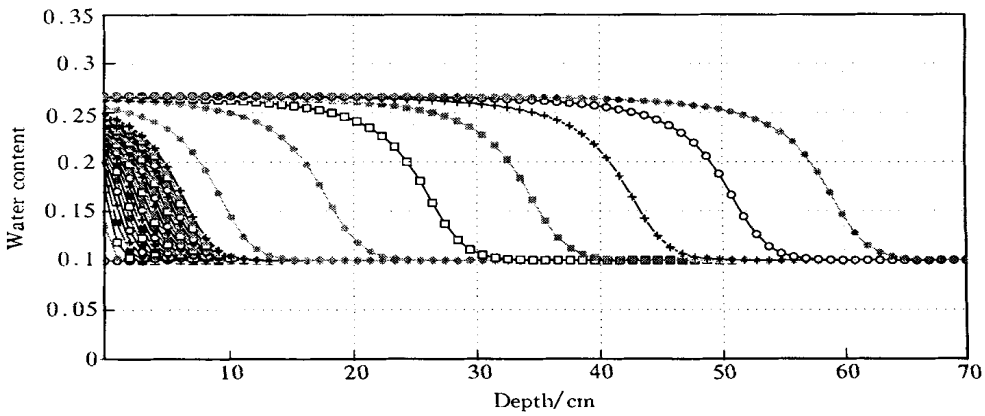

Fig. 2. Soil moisture profiles in initial stage and at each 0.1 h afterwards.

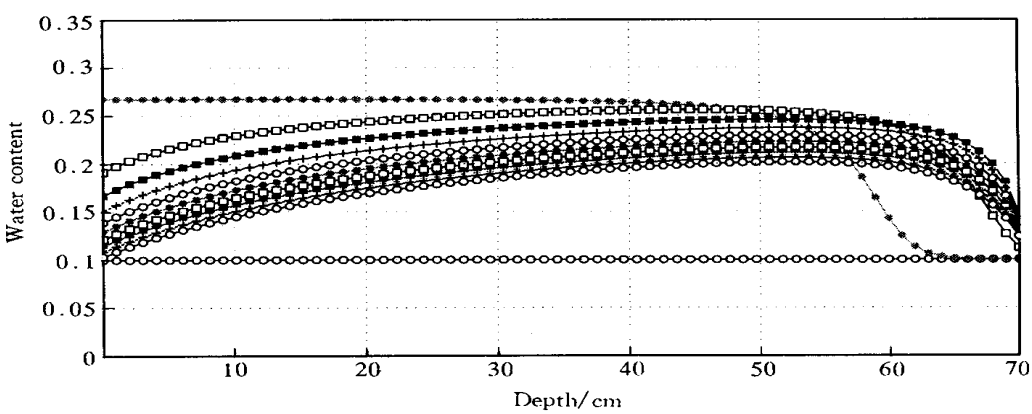

Fig. 3. Infiltration, evaporation, air-drying for soil at surface.

each 0.1 period afterwards. Fig. 3 shows that when evaporation began, soil moisture at surface decreased. Because of the gravity flow, the front of soil moisture approaching the lower boundary moved forward. After 0.1 h since beginning of evaporation, soil moisture profiles decreased with time levels. Finally, soil moisture at surface reached the air-dried rate 0.1 at the 1 200th level, i.e. about 1.67 h, and soil moisture approaching the lower boundary gradually approximated to the air-dried rate 0.1. This shows that the numerical model simulated very well infiltration, evaporation, evapotranspiration, re-distribution, and their alternate appearances.

© 1995-2004 Tsinghua Tongfang Optical Disc Co., Ltd. All rights reserved.

We now discuss mass conservation. The balance error for the ith level is defined by $BE(t^j) = abs(1 - MB(t^j))$, where

$$MB(t^j) = \frac{\left\{ \sum_{i=1}^{n-1} [(\theta_i - \theta_i^0)(\Delta z)] + \left(\theta_0 - \theta_0^0\right)\left(\frac{\Delta z}{2}\right) + \left(\theta_n - \theta_n^0\right)\left(\frac{\Delta z}{2}\right) \right\}}{\left\{ \sum_{=1}^{j} (q_0^i - q_N^i)\Delta t \right\}}.$$

Fig. 4 presents the balance error dependent on time level. From the figure, it may be seen that at the initial stage, the balance error exceeded 9 %, and then decreased rapidly. It decreased below 2 % at 180th level, below 1.5 % after 260th level. Hence it has a good mass-conservative property.

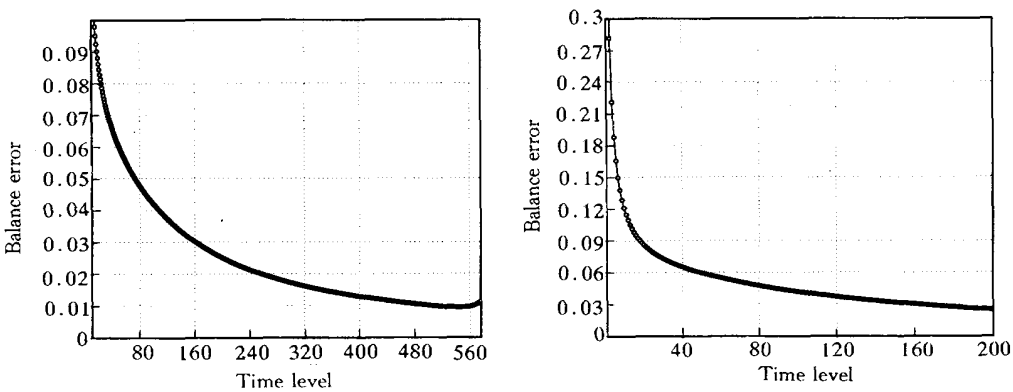

Fig. 4. Balance error dependent on time level.

Iteration number with time level is presented in fig. 5, which shows that iteration number at initial stage changed from 8, 5 to 4, and kept 3 after 80 time-level. This shows that the numerical model is provided with good convergence and stability, but that at initial stage iteration number was larger, which coincides with our scheme and may be explained in the following analysis. In computation, the next level water head is pre-estimated through a linear extrapolation of the recent two-level water head, and then the correct iteration is done from the pre-estimated result. In this case, the estimate of coefficients about time variable is the second-order precision. However, that at initial moment is the first-order precision in this case, the linear extrapolation cannot be done and the next level water head was pre-estimated through explicit extrapolation i.e. using the known initial water head profile and the relative soil parameter profile, and then correct iteration was done as the previous case. It is natural to need more iterations in this case. It follows

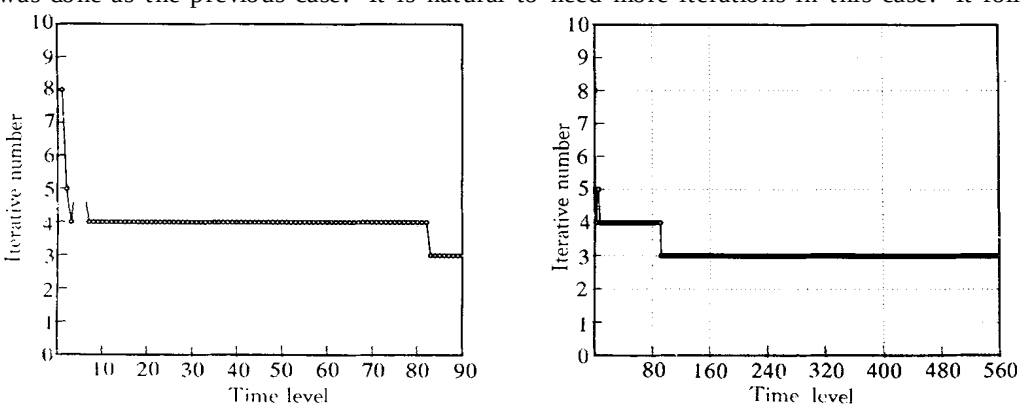

Fig. 5. Iteration number dependent on time level.

© 1995-2004 Tsinghua Tongfang Optical Disc Co., Ltd. All rights reserved.

that the shorter the time step is, the better the pre-estimated effect will be.

3 Conclusions and discussions

A numerical model for the *h*-form unsaturated flow problem by using the mass-lumped finite element method is established in order to simulate liquid moisture flow in unsaturated zone with homogeneous soil and deep subsurface water, and under different initial and boundary conditions. Infiltration and evaporation boundary conditions are handled through reducing to calculation of known boundary flux by using variation. It demonstrated an easy and good treatment. At each new time step, the water head distribution is pre-estimated through linear extrapolation from the old distribution, and then is solved by the correct iteration, which can reduce iteration number. Numerical results show that the model evades oscillatory non-physics solutions by using the mass-lumped finite element method, and can be used in numerical simulation of liquid moisture flow for infiltration, evaporation, evapotranspiration, re-distribution, and their alternate appearances, and that the scheme possesses a good mass-conservative property, convergence and stability of pre-estimation and iterative correction. Numerical simulation of the unsaturated flow problem has a significance in improving calculation of soil water flow and soil temperature in land parameterization, and working in effect on the source of groundwater caused by climate change. Convergence and error analysis of the mass-lumped finite element approximation scheme will be discussed in another paper. Numerical simulation of saturated-nonsaturated problems with shallow subsurface, especially subsurface problem, will be studied further.

References

1 Ye Duozheng, Zeng Qingcun, Guo Yufu, *Model Climate Studies* (in Chinese), Beijing: Climate Press, 1991, 236—261.
2 Dai Yongjiu, Zeng Qingcun, A land surface model (IAP94) for climate studies, Part I: Formulation and Validation in off-line experiment, *Advances in Atmospheric Sciences*, 1997, 14(4): 433.
3 Lei Zhidong, Yang Shixiu, Xie Songcuan, *Soil Hydrology* (in Chinese), Beijing: Tsinghua University Press, 1988, 270—319.
4 Bear, J., *Dynamics of Fluids in Porous Media*, New York: American Elsevier Publishing Company Inc., 1972.
5 Celia, M. A., Boulouton, E. T., Zarba, R. L., A general mass conservation numerical solution for the unsaturated flow equation, *Water Resour. Res.*, 1990, 26(7): 1483.
6 Klaus, R. Linda, M. A., Mass conservative numerical solutions of the head-based Richards equation, *Water Resour Res.*, 1994, 30(9): 2579.
7 Haverkamp, R., Vauclin, M., Touma, J. et al., A comparsion of numerical simulation models for one-dimensional infiltration, *Soil Sci. Soc. Am. J.*, 1977, 41: 285.
8 Watson, K. K., An instantaneous profile method for determining the hydraulic conductivity of unsaturated porous material, *Water Pesour. Res.*, 1968, 2: 709.
9 Vachaud, G., Thony, J. L., Hysteresis during infiltration and redistribution in a soil column at different initial water contents, *Water Resour. Res.*, 1971, 7: 111.
10 Adams, R. A., *Sobolev Spaces*, New York: Academic Press, 1975, 26—74.
11 Ciarlet, P. C., *The Finite Element Methods for Elliptic Problems*, Amsterdam: North-Holland, 1978, 1—50.

© 1995-2004 Tsinghua Tongfang Optical Disc Co., Ltd. All rights reserved.